15TH IEA HEAT PUMP CONFERENCE
MAY 26–29, 2026 | HOFBURG
VIENNA 2026
DECARBONISATION THROUGH INNOVATION

Field-based and predictive assessment of effective borehole thermal resistance in standing column wells

Gabrielle Beaudry[a,*], Philippe Pasquier[a], Louis Jacques[b]

[a]Polytechnique Montréal, 2500 Chemin De Polytechnique, Montréal H3T1J4, Canada
[b]CanmetÉNERGIE, 1615 Bd Lionel-Boulet, Varennes J3X1P7, Canada

Abstract

Standing column wells (SCWs) are ground heat exchangers that operate by recirculating groundwater in a deep uncased borehole and by bleeding a fraction of the water to stimulate advection during peak periods. While the high efficiency of SCWs is well recognized, the methodology to characterize their effective borehole thermal resistance remains poorly documented. To address this gap, an analysis was performed using data from 80-h thermal response tests conducted on eight SCWs across the St. Lawrence Lowlands in Canada. The no-bleed phase of each test was analysed using line-source theory, and effective borehole thermal resistance values were inferred under uncertainty in a Bayesian framework. Results show that the inferred resistance range (0.005 to 0.025 m·°C/W) is markedly lower than that typically observed in conventional closed-loop boreholes, highlighting the thermal performance of SCWs. The comparison with predictions from the only existing theoretical formulation yielded a similar range (0.004 to 0.029 m·°C/W), with predicted values allowing to reproduce the no-bleed behaviour of SCWs with a mean relative error below 1% in seven out of eight wells. These findings provide the first integrated field-based and predictive assessment of effective borehole thermal resistance in SCWs. They demonstrate that precise estimation of this parameter can reliably reproduce SCW thermal behaviour during conduction-dominant operation and highlight its potential to support computationally efficient design tools.

Standing column wells; Effective borehole thermal resistance; Thermal response test; Bayesian inference.

1. Introduction

Standing column wells (SCWs) are efficient ground heat exchangers that recirculate groundwater within a deep and uncased borehole. During periods of peak thermal demand, bleeding, or withdrawing a small fraction of the circulated water, can enhance performance by renewing the well water and promoting advective heat transfer. Although the high efficiency of SCWs is well established, accurately predicting their thermal response remains challenging due to the coupled effects of conductive and advective heat transfer [1,2,3]. In the past decades, several studies have addressed this challenge by developing and experimentally validating numerical models [4,5,6,7]. However, these models require substantial computational resources and development effort, which limit their practicality during design phases and hinder wider adoption by practitioners.

To overcome these limitations, recent studies have focused on developing agile and computationally efficient analytical models capable of simulating the thermal behaviour of SCWs operating with bleed [8,9]. The improved model proposed by Jacques et al. [9], building on the earlier work of Nguyen et al. [8], is a notable contribution that allows predicting the outlet fluid temperature, which is the primary design parameter required for integration into sizing algorithms [10]. A key feature of this model is its use and novel formulation of the effective borehole thermal resistance. Unlike the local borehole thermal resistance, which characterizes heat transfer at a specific depth, the effective fluid-to-ground resistance accounts for performance losses caused by short-circuiting between the downward and upward flow segments within the borehole. This effective

* Corresponding author. *E-mail address:* gabrielle.beaudry@polymtl.ca

resistance formulation thus captures internal borehole effects and enables direct prediction of the outlet fluid temperature, making it better suited for implementation in design tools and simulation platforms [11,12].

The concept of effective borehole thermal resistance is well documented for conventional grouted boreholes [11,13,14], concentric configurations [15], and groundwater-filled closed-loops [16,17]. However, only a limited number of studies have examined this concept for SCWs. Deng [18] first proposed a method to predict the local borehole thermal resistance and estimate the additional temperature difference due to thermal short-circuiting. Jacques et al. [9] later provided the first full formulation of the effective borehole thermal resistance for SCWs, adapting a model originally developed for concentric closed-loop boreholes with uniform heat flux along the depth. While experimental data were used to validate their analytical model, the predicted effective resistance values themselves were not specifically analysed or independently verified. To the authors' knowledge, the only experimental evaluations of effective borehole thermal resistance in SCWs are those reported by Chang et al. [19,20], and You and Lee [21]. Using the infinite line source (ILS) model to invert data from 12-24 h thermal response tests (TRTs), these studies provided a first empirical range, approximately 0.003-0.012 m·°C/W. They also emphasized the strong dependence of resistance values on borehole depth and flow rate, underscoring the need for further investigation. However, uncertainty was not quantified, nor were the measured values compared with theoretical predictions.

The present work aims to conduct a combined investigation of the existing field-based and predictive approaches for evaluating the effective borehole thermal resistance in SCWs, with the goal of providing a first assessment of their adequacy and reliability. The study is structured in three parts. First, a series of 80-h TRTs was performed on eight SCWs of varying depths and located in diverse hydrogeological contexts, providing high-quality experimental data. Second, these data were used to infer the effective borehole thermal resistance of the eight SCWs using the ILS model in a Bayesian framework to quantify the associated uncertainty. Finally, theoretical predictions of the resistance for the eight SCWs were computed using the formulation of Jacques et al. [9], enabling a first assessment of its alignment with the existing empirical approach.

2. Methods

The effective borehole thermal resistance was investigated in eight SCWs located across the St. Lawrence Lowlands, one of Canada's most densely populated regions. This section outlines the procedures for the 80-hour TRTs performed on these SCWs, the method used to invert the data and derive field-based estimates of the effective resistance, and the predictive model for computing comparative theoretical values. Finally, the Bayesian framework used to quantify the uncertainty of the empirical estimates is described.

2.1. Field testing

A dedicated TRT rig was specifically developed for SCWs. The system, designed at Polytechnique Montréal, is housed in an insulated trailer equipped with a 29-kW water heater, two electromagnetic flowmeters (±0.5 % accuracy), and redundant temperature probes (±0.25 °C accuracy). All internal piping and components are made of copper, grade 316 stainless steel, or brass, to minimize chemical reactivity with groundwater, and the piping is thermally insulated to reduce conductive and radiative heat losses. A 1.5 HP submersible pump was installed in the SCWs at approximately 20 m depths, typically 10 m below the expected minimum groundwater level. An HDPE pipe (⌀5.1-7.8 cm) was installed in the wells to allow reinjection at the bottom while maintaining a 10-m sedimentation chamber. External pipes connecting the well and the trailer were wrapped in insulation blankets to minimize thermal losses. All equipment was disinfected with a sodium hypochlorite solution prior to mobilization to prevent cross-contamination between sites. The testing procedure typically comprised four main phases:

- Constant-rate recirculation (~24 h);
- Constant-rate recirculation with heat injection (~80-115 h);
- Constant-rate recirculation with heat injection and bleed (~24 h);
- Constant-rate recirculation with bleed (~24 h).

The circulation flow rate for the recirculation phase was typically 130 L/min, determined by the pump capacity. An average heating power of 27 kW was applied to ensure a clear thermal signal relative to background noise. Note that this value is higher than in conventional TRTs on closed-loop boreholes, due to the greater depth and thermal inertia of SCWs. Although not considered in the present work, most tests included a bleed phase, performed by diverting part of the pumped water to a storm drain, to assess whether it could improve thermal performance. Throughout testing, measurements of pumping and bleed flow rates, and groundwater temperatures at the borehole inlet and outlet were recorded at one-minute intervals.

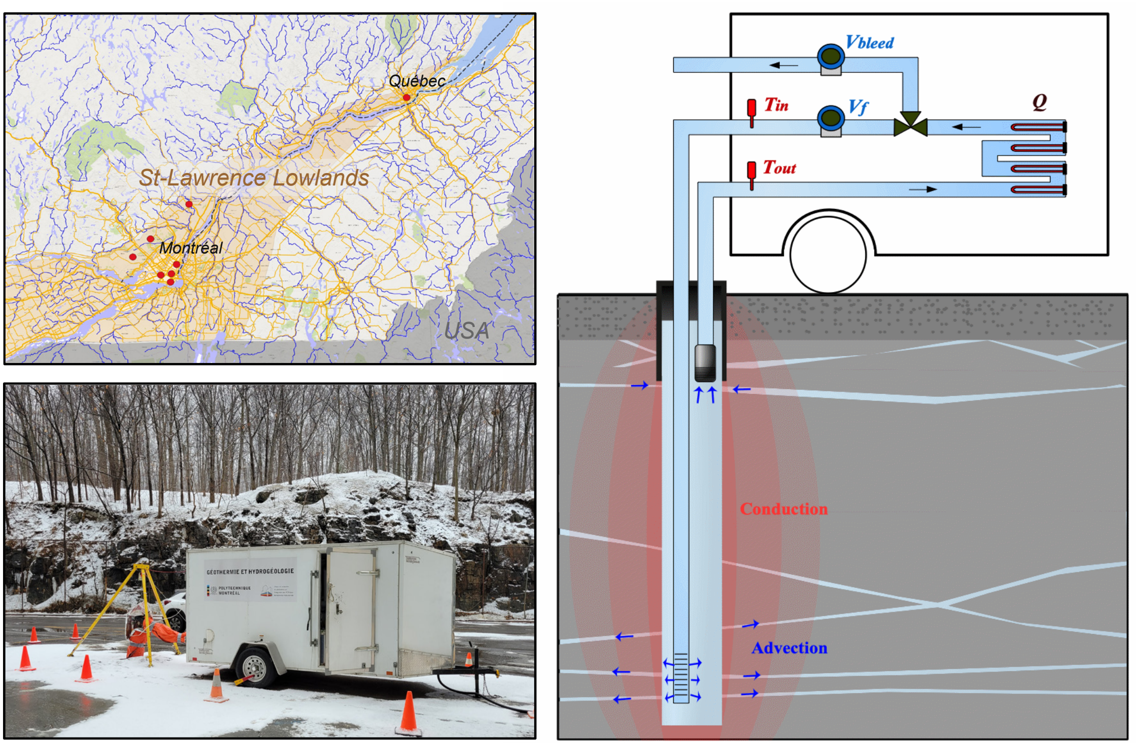

Fig. 1. Location of the eight test sites (top left), photograph of the TRT rig (bottom left), and its schematic (right).

2.2. Field-based effective borehole thermal resistance

In this exploratory study, the TRT data described in the previous section were implemented in Eq. 1 to determine the experimental effective borehole thermal resistance R_b^* of the tested SCWs [14]:

$$T_f(t) = T_0 + \Delta T_b(t) + q_b R_b^*(t) \tag{1}$$

The fluid temperature T_f was defined as the arithmetic mean of the inlet (T_{in}) and outlet (T_{out}) temperatures of the borehole [12]. The undisturbed temperature T_0 was taken as the fluid temperature at the onset of the heating phase of the TRT.

The mean heat transfer rate during the heating phase q_b was evaluated using Eq. 2, where V_f is the circulation flow rate inside the SCW, C_f is the volumetric heat capacity of the circulating groundwater, and H is the height of the water column contributing to heat transfer:

$$q_b = V_f C_f (T_{in} - T_{out})/H \tag{2}$$

The mean borehole wall temperature rise ΔT_b was estimated using the simplified ILS solution [22]:

$$\Delta T_b(t) = \frac{q_b}{4\pi k_r^*}\left[ln\left(\frac{4\alpha t}{r_b^2}\right) - \gamma\right] \tag{3}$$

where α is the ground's thermal diffusivity, r_b is the borehole's radius, γ is the Euler's constant, and k_r^* is the effective thermal conductivity of the ground. The latter was evaluated from each TRT dataset using the first-order approximation of the ILS model [23]:

$$k_r^* = \frac{q_b}{4\pi m} \quad \text{where} \quad m = \frac{\delta(T_f(t))}{\delta(ln(t))} \quad \text{for} \quad t \geq 5r_b^2/\alpha \tag{4}$$

Note that this simplified ILS formulation, which remains the only method applied to date for evaluating effective borehole resistance in SCWs [19-21], was selected to provide an initial assessment of its consistency with theoretical predictions. Its computational efficiency also made it suitable for conducting a robust uncertainty analysis, as described in Section 2.4. The underlying assumptions, including the representation of heat transfer as purely conductive, should however be acknowledged, as they may limit its accuracy for SCWs and highly transmissive formations where advective effects are significant. At last, the effective borehole thermal resistance R_b^* was obtained as the mean stabilized value of $R_b^*(t)$ during the heating phase for $t \geq 5r_b^2/\alpha$, as defined in Eq. 1.

2.3. Theoretical effective borehole thermal resistance

The theoretical effective borehole thermal resistance of the eight tested SCWs was predicted using the formulation of Jacques et al. [9]. In this approach, the SCW is modelled as a concentric ground heat exchanger, allowing the effective fluid-to-ground resistance to be represented as the network of internal heat transfer resistances illustrated in Fig. 2. Building on Hellström's [11] formulation for grouted closed-loop boreholes and Lamarche's [15] extension for concentric configurations, and assuming a uniform heat flux at the borehole wall, the effective borehole thermal resistance R_b^* of the SCW is expressed as:

$$R_b^* = R_{C,b} \cdot \left(1 + \frac{R_v^2}{3R_a R_{C,b}}\right) \tag{5}$$

where R_a accounts for short-circuiting between the downward and upward groundwater in the borehole, and R_v introduces the influence of the height of the water column contributing to heat exchange with the ground:

$$R_v = \frac{H}{C_f V_f} \tag{6}$$

$$R_a = R_{C,o} + R_p + R_{C,i} \tag{7}$$

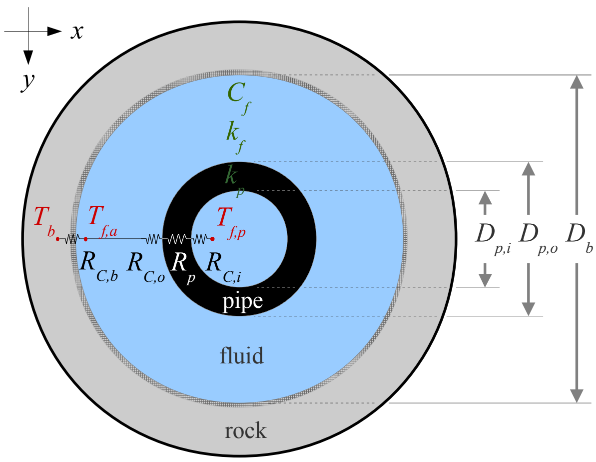

Fig. 2. Thermal resistance network representing the internal resistances of a SCW, adapted from Jacques et al. [9].

In Eq. 5-7, $R_{C,b}$, $R_{C,o}$, and $R_{C,i}$ are the convective film resistances at the interfaces between the circulating groundwater and the borehole wall, the outside pipe wall, and the inside pipe wall, respectively, while R_p represents the conductive resistance of the pipe:

$$R_{C,b} = \frac{1}{2\pi r_b h_b} \quad \text{with} \quad h_b = \frac{Nu_b \cdot k_f}{2r_h} \tag{8}$$

$$R_{C,o} = \frac{1}{2\pi r_{p,o} h_{p,o}} \quad \text{with} \quad h_{p,o} = \frac{Nu_{p,o} \cdot k_f}{2r_h} \tag{9}$$

$$R_{C,i} = \frac{1}{2\pi r_{p,i} h_{p,i}} \quad \text{with} \quad h_{p,i} = \frac{Nu_{p,i} \cdot k_f}{2r_{p,i}} \tag{10}$$

$$R_p = \frac{1}{2\pi k_p} ln\left(\frac{r_{p,o}}{r_{p,i}}\right) \tag{11}$$

where $r_h = r_b - r_{p,o}$ is the hydraulic radius of the annulus, h denotes the convective heat transfer coefficient, and Nu is the Nusselt number. In this study, Nu was calculated following the suggested approach of Jacques et al. [9]: the Dittus–Boelter correlation was applied for turbulent flow ($Re > 10000$), while the Gnielinski correlation was used for transitional flow ($2300 < Re < 10000$) [24]. For the latter, the Darcy friction factor was evaluated using the Colebrook-White equation [25]. This framework provides a consistent theoretical prediction of R_b^* for SCWs, allowing direct comparison with the field-based estimates.

2.4. Uncertainty analysis

The uncertainty associated with the field-based estimates of the effective borehole thermal resistance was quantified using a Bayesian framework adapted from Pasquier and Marcotte [26] and Jacques and Pasquier [27]. This framework was used to infer the marginal and joint distributions of the underground thermal conductivity k_r^* and effective borehole thermal resistance R_b^*, given observations of the mean fluid temperature T_f and a set of latent variables (C_r, T_0, q_b, r_b) required to solve the ILS model. According to Bayes' theorem, the posterior distribution $P(\theta \mid x)$ is proportional to the product of the likelihood $P(x \mid \theta)$ and the prior distribution $P(\theta)$:

$$P(\theta|x) \propto P(x|\theta) \cdot P(\theta) \tag{12}$$

In this study, the parameter vector is $\theta = [k_r^*, R_b^*, C_r, T_0, q_b, r_b]$, and the observation vector x contains the model residuals $\tilde{T}_f(t) - T_f(t)$. The prior distribution $P(\theta)$, representing our beliefs about the true parameter values, is assumed to follow independent truncated uniform distributions (Eq. 13) for k_r^*, R_b^*, and C_r, while the latent variables T_0, q_b, and r_b follow truncated Gaussian distributions (Eq. 14) with mean μ and standard deviation σ.

$$P(\theta) = \begin{cases} \prod_{i=1}^{p} \frac{1}{b_i - a_i} & \text{if } \theta_i \in [a_i, b_i] \\ 0 & \text{otherwise} \end{cases} \tag{13}$$

$$P(\theta) = \begin{cases} \frac{\varphi(\xi_i)}{\sigma(\Phi(\beta_i) - \Phi(\alpha_i))} & \text{if } \theta_i \in [a_i, b_i] \\ 0 & \text{otherwise} \end{cases} \tag{14}$$

Here, a_i and b_i denote the lower and upper bounds of each parameter i, and the probability density function φ (Eq. 15) and cumulative distribution function Φ (Eq. 16) are expressed in terms of the standardized variables $\xi = (x - \mu)/\sigma$, $\alpha = (a - \mu)/\sigma$, and $\beta = (b - \mu)/\sigma$.

$$\varphi(\xi) = \frac{1}{\sqrt{2\pi}} exp\left(-\frac{1}{2}\xi^2\right) \tag{15}$$

$$\Phi(\alpha, \beta) = \frac{1}{2}\left(1 + erf\left(\alpha, \beta/\sqrt{2}\right)\right) \tag{16}$$

The likelihood $P(x \mid \theta)$ quantifies the probability of observing x given the model parameters θ, and serves to update prior knowledge with experimental evidence. Its expression is given by Eq. 17, assuming a multi-Gaussian distribution and accounting for the autocorrelation of the residuals x.

$$P(x|\theta) = (2\pi)^{-n/2} |\Sigma|^{-\frac{1}{2}} e^{-\frac{1}{2}x'\Sigma^{-1}x} \tag{17}$$

where $|\Sigma|$ and Σ^{-1} are the determinant and inverse of the $n \times n$ covariance matrix. To reduce the computational cost, both were evaluated using the closed-form solution of Pasquier and Marcotte [26].

Throughout the inference process, the posterior distribution $P(\theta \mid x)$ was sampled using a Markov Chain Monte Carlo (MCMC) algorithm, specifically the ensemble slice sampler of Karamanis and Beutler [28]. This method runs multiple chains in parallel, generating samples that iteratively converge to the true posterior. The ensemble structure allows collective adaptation of sampling direction and step size, improving efficiency and convergence compared to single-chain MCMC. In this study, 50 parallel chains were used to ensure thorough exploration of the parameter space and robust estimation of the posterior distribution.

3. Results and discussion

The following section presents the outcomes of the inference process used to estimate the effective borehole thermal resistance of the eight SCWs under uncertainty. The theoretical values from the predictive formulation of Jacques et al. [9] are then compared with the inferred results to assess the adequacy of both methods.

3.1 Experimental parameters inference

Table 1 summarizes all inputs used to define the prior distributions in the Bayesian framework. The bounds of the uniform prior distributions for the unknown thermal parameters (ground thermal conductivity k_r^*, borehole thermal resistance R_b^*, and ground volumetric capacity C_r) are first displayed. The mean and standard deviation of the Gaussian priors assigned to the measured parameters (initial ground temperature T_0, heat transfer rate q_b, and well radius r_b) are then provided. The means were deduced from experimental measurements, and the standard deviations were calculated using the error-propagation method described in Moffat [29], which systematically combines the effects of individual measurement errors to determine the overall parameter uncertainty. It should be noted that the uncertainties assigned to the priors were deliberately allowed a wide range to provide a conservative assessment of the resulting posterior uncertainties. Finally, the lower bound of the Gaussian distribution for r_b was constrained by the measured diameter of the drilling bit.

Table 1. Definition of the prior distributions used in the Bayesian framework.

	Bounds of the uniform prior distributions			**Mean and standard deviation of the gaussian prior distributions**		
SCW	k_r^* W/(m·ºC)	R_b^* m·ºC/W	C_r MJ/(m³·ºC)	T_0 °C	q_b W/m	r_b m
1	1-5	0.001-0.060	1.9 - 2.7	11.9 ± 0.1	45 ± 3	0.092 ± 0.005
2	1-5	0.001-0.060	1.9 - 2.7	10.1 ± 0.1	34 ± 3	0.090 ± 0.005
3	1-5	0.001-0.060	1.9 - 2.7	11.7 ± 0.1	38 ± 4	0.082 ± 0.005
4	1-5	0.001-0.060	1.9 - 2.7	11.0 ± 0.1	47 ± 4	0.083 ± 0.005
5	1-5	0.001-0.060	1.9 - 2.7	9.7 ± 0.1	42 ± 5	0.083 ± 0.005
6	1-5	0.001-0.060	1.9 - 2.7	9.6 ± 0.1	61 ± 5	0.082 ± 0.005
7	1-5	0.001-0.060	1.9 - 2.7	11.5 ± 0.1	59 ± 6	0.084 ± 0.005
8	NA	0.001-0.060	1.9 - 2.7	8.9 ± 0.1	154 ± 17	0.088 ± 0.005

Next, Fig. 3 presents the prior and marginal posterior distributions of the inferred parameters for the eight SCWs. Although wide uniform priors were assigned to k_r^* and R_b^*, the resulting posterior distributions appear to follow a Gaussian behaviour confined to a much narrower range. The inference process was thus successful in providing robust estimates of these properties, even when using the simple ILS model. However, large standard deviations are observed for the inferred R_b^* values, ranging from 21 % to 52 % of the mean estimates. In contrast, the parameter C_r, which was also assigned a uniform prior, shows little to no improvement in its posterior distribution. This limited identifiability can be attributed to the weak influence of C_r within the forward ILS model and suggests that more advanced tools, such as the improved analytical model of Jacques et al. [9] or a numerical model, may be required to better constrain this parameter. The remaining posterior distributions of latent variables T_0, q_b, and r_b remain strongly shaped by their Gaussian priors.

Lastly, Fig. 4 compares the measured temperature rise in the SCWs with the modelled temperatures obtained using the ILS model and the inferred parameters. The low mean relative errors (MREs) for SCW-1 to SCW-7, all below 1.0 %, indicate that heat transfer during the heating phases of the TRTs was predominantly conductive and that the ILS model effectively captures the main thermal processes on this timescale. In contrast, the agreement for SCW-8 is significantly poorer (MRE = 6.1 %), which can be traced to the inference process failing to produce a coherent estimate of the ground thermal conductivity, as shown in Fig. 3. This suggests that conductive heat transfer was not the dominant mechanism at this site, and underscores the limitations of the current approach, which are discussed in the following sections.

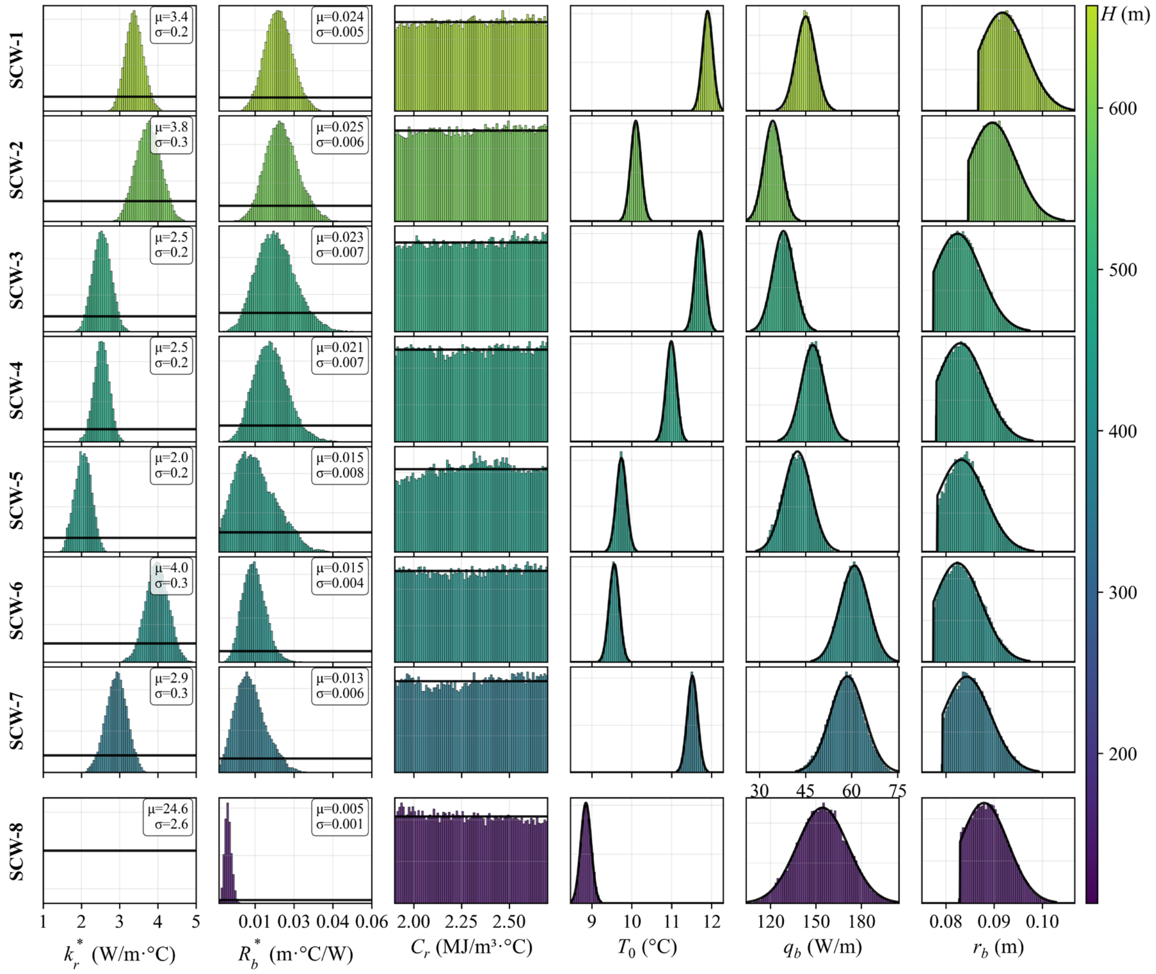

Fig. 3. Marginal probability distributions inferred for TRTs conducted on eight SCWs characterized by an effective heat exchange height H. Black lines represent prior distributions; coloured histograms show posteriors, with mean (μ) and standard deviation (σ) values for the main parameters.

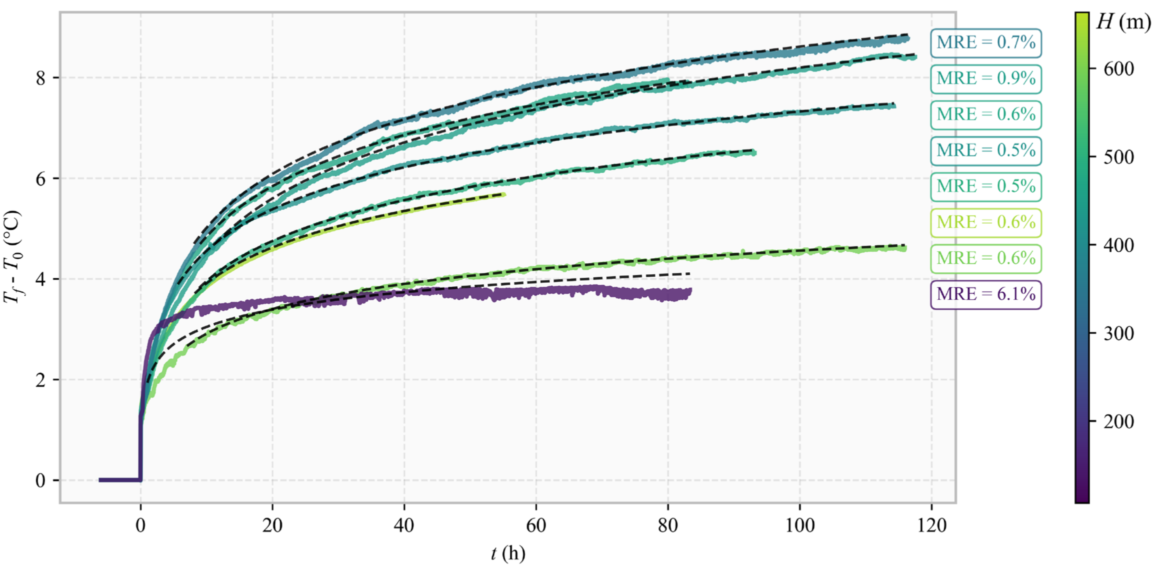

Fig. 4. Temperature rise in the SCWs characterized by an effective heat exchange height H: temperature measured during the TRTs (coloured lines) and modelled by the ILS using the inferred parameters (black dashed lines).

3.2 *Effective borehole thermal resistance*

Table 2 reports the inferred mean values of k_r^* and R_b^* and their associated standard deviations, along with the corresponding theoretical predictions of R_b^* obtained using the model of Jacques et al. [9]. The table also includes several auxiliary parameters that help contextualize the results. Specifically, it presents H, the height of the water column contributing to heat exchange within the borehole; V_f, the circulation flow rate in the SCW; and T, the transmissivity of the surrounding hydrogeologic formation, determined from independent pumping tests.

Table 2. Inferred and predicted effective borehole thermal resistance values for the eight tested SCWs.

SCW	H m	V_f L/min	T m²/s	k_r^* (exp) W/m·°C	R_b^* (exp) m·°C/W	R_b^* (theo) m·°C/W
1	638	149	4.4e-04	3.4 ± 0.2	0.024 ± 0.005	0.024
2	590	126	3.4e-05	3.8 ± 0.3	0.025 ± 0.006	0.029
3	492	122	1.2e-04	2.5 ± 0.2	0.023 ± 0.007	0.021
4	470	123	1.2e-05	2.5 ± 0.2	0.021 ± 0.007	0.019
5	445	125	2.3e-07	2.0 ± 0.2	0.015 ± 0.008	0.017
6	419	128	6.6e-03	4.0 ± 0.3	0.015 ± 0.004	0.015
7	356	130	2.3e-04	2.9 ± 0.3	0.013 ± 0.006	0.011
8	133	128	7.9e-03	NA	0.005 ± 0.001	0.004

The results show that the inferred effective borehole resistances range from 0.005 to 0.025 m·°C/W, closely matching the theoretical predictions, which span 0.004 to 0.029 m·°C/W. This correspondence is more clearly illustrated in Fig. 5, which plots the inferred effective resistance values against their theoretical counterparts. As expected from the predictive model (Eqs. 5-6), the resistance tends to increase with the height of the heat exchange H, due to short-circuiting between the upward and downward segments. The only notable exception is SCW-1, which exhibits a lower resistance than SCW-2 despite its greater depth. This discrepancy is explained by the second most influential parameter, the circulation flow rate V_f, which increases turbulence and reduces film convective resistance between the groundwater and the borehole wall.

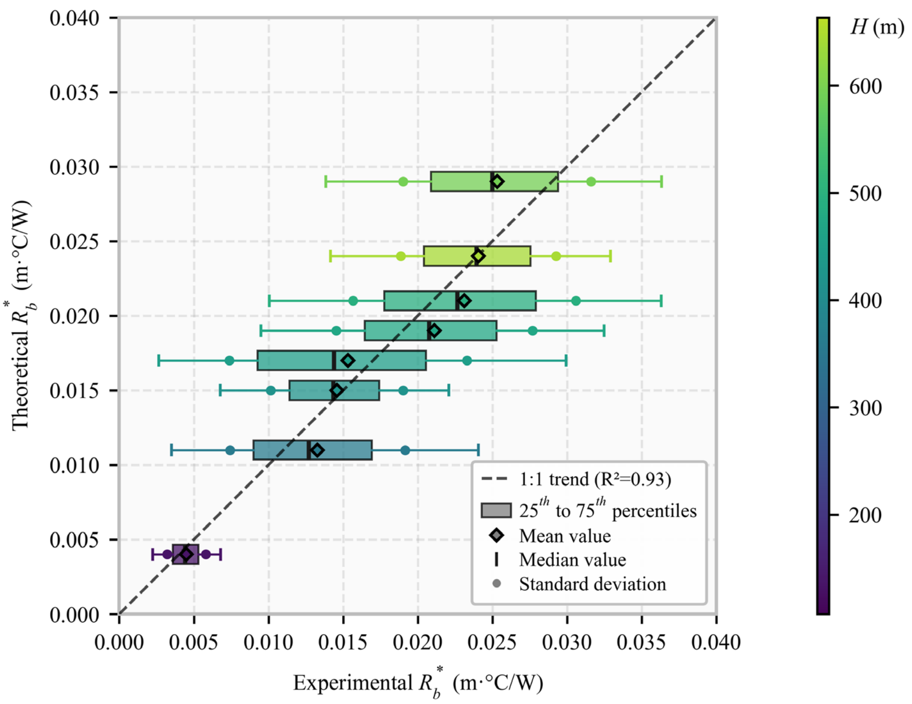

Fig. 5. Comparison of experimental and theoretical effective borehole thermal resistance R_b^* in the eight tested SCWs, and corresponding effective heat exchange height H. Boxplots show the inferred distributions of experimental estimates, with whiskers representing a 95 % confidence interval.

3.3 Discussion

A first observation concerns the range of effective borehole thermal resistance values inferred experimentally (0.005-0.025 m·°C/W) and predicted theoretically (0.004-0.029 m·°C/W) for the eight tested SCWs. These values are markedly lower than those typically reported for conventional closed-loop systems, which generally range from 0.050 to 0.130 m·°C/W, even though such boreholes are usually much shorter [12]. This contrast underscores the high thermal efficiency of SCWs, which arises from the direct contact between circulating groundwater and the borehole wall and the large groundwater volume within the well (up to 11 m^3 for a 600 m borehole), which acts as a substantial thermal buffer.

The agreement between inferred and predicted resistances (Fig. 5), as well as the accurate reproduction of the measured temperatures (Fig. 4), suggest that the ILS model and the theoretical formulation of the effective borehole thermal resistance proposed by Jacques et al. [9] capture the dominant heat transfer processes occurring within the SCWs during the reported TRTs. Nevertheless, it is important to emphasize that this correspondence is obtained within a simplified modelling framework, which partly explains the relatively large uncertainties of the inferred resistance estimates. Although the Bayesian implementation of the ILS model provides a computationally efficient means of quantifying uncertainty, it simplifies several key aspects of borehole thermal behaviour, including thermal short-circuiting, water residence time, non-uniform undisturbed bedrock temperature, and radial advective fluxes.

The limitations of this framework are illustrated by SCW-8, for which Tables 1 and 2 do not display the inferred value of k_r^*, as it falls outside the physically attainable range. This arises from the incapacity of the ILS model to capture the effects of the high bedrock transmissivity, which induces dominant advective thermal exchange even without bleed [30]. The effective borehole resistance of SCW-8 is nevertheless presented because it remains consistent with the overall trend observed across the wells, supporting the general relevance of the approach. In the future, a more advanced simulation framework, such as the improved analytical model of Jacques et al. [9] or a fully numerical model, will be required to improve estimation precision and to verify the theoretical formulation of borehole thermal resistance in SCWs under advective-dominant conditions.

4. Conclusion

This exploratory study presented a combined field-based and predictive assessment of effective borehole thermal resistance in SCWs, aiming to evaluate the adequacy and reliability of existing approaches. A series of 80-h TRTs were conducted on eight SCWs of varying depths and hydrogeological contexts, providing high-quality experimental data. These data were then used to infer the effective borehole thermal resistance under uncertainty, using the ILS model in a Bayesian framework, while independent theoretical predictions were obtained using the formulation proposed by Jacques et al. [9]. The resulting inferred resistance values (0.005 to 0.025 m·°C/W) showed good agreement with the theoretical predictions (0.004 to 0.029 m·°C/W), and both methods captured expected physical trends. Namely, an increase in resistance associated with greater borehole depth and reduced flow rates was observed. The inferred resistances also enabled accurate reproduction of the no-bleed temperatures in seven of the eight SCWs where conduction was the dominant heat transfer mechanism. These results provide the first integrated field-based and predictive assessment of effective borehole thermal resistance in SCWs and simultaneously demonstrate the high thermal efficiency of these systems, which exhibit markedly lower resistance values than conventional closed-loop boreholes despite having greater depths.

Some inherent limitations of the proposed approach were highlighted by the results of this exploratory study. While the ILS model proved to be a flexible and effective tool for assessing uncertainty within a Bayesian framework, it yielded inferred resistance values with relatively large standard deviations (21% to 52%). Furthermore, the inference process resulted in other latent variables, such as ground thermal capacity, remaining largely shaped by their priors. Together, these results suggest a limited parameter identifiability inherent in the ILS model, which becomes particularly evident in advection-dominant scenarios.

Ultimately, the findings of this study indicate that the effective borehole thermal resistance is a promising metric for efficient and reliable SCW simulation. To improve estimation precision and applicability in advection-dominant scenarios, future research should focus on assessing effective borehole thermal resistance using advanced models that incorporate groundwater advection, borehole thermal capacity and geometry, while rigorously quantifying uncertainties. These efforts should allow improving predictive capability and support robust and efficient SCW design across diverse hydrogeological contexts.

Acknowledgements

The authors wish to thank the anonymous reviewers for their helpful comments and suggestions.

References

[1] S. J. Rees, J. D. Spitler, Z. Deng, C. D. Orio, and C. N. Johnson, « A study of geothermal heat pump and standing column well performance », *ASHRAE Transactions*, vol. 109, nº 1, p. 3-13, 2004.

[2] C. D. Orio and Z. J. Patnaude, « Eight years of operation of 615-ton geothermal nursing home in Northern Tier », *ASHRAE Transactions*, vol. 120, nº 8, 2014.

[3] G. Beaudry, J. Faucher, G. Tonellato, P. Pasquier, and M. Kummert, « Standing column wells in cold climates: lessons learned after one year of operating a demonstration system in Canada », in *2024 Research Conference Proceedings of the IGSHPA*, International Ground Source Heat Pump Association, 2024.

[4] Z. Deng, S. J. Rees, and J. D. Spitler, « A model for annual simulation of standing column well ground heat exchangers », *HVAC&R Research*, vol. 11, nº 4, p. 637-655, 2005.

[5] B. M. Ng, C. P. Underwood, and S. L. Walker, « Standing column wells—Modeling the potential for applications in geothermal heating and cooling », *HVAC&R Research*, vol. 17, nº 6, p. 1089-1100, 2011.

[6] G. Beaudry, P. Pasquier, and D. Marcotte, « The impact of rock fracturing and pump intake location on the thermal recovery of a standing column well: model development, experimental validation, and numerical analysis », *Science and Technology for the Built Environment*, vol. 25, nº 8, p. 1052-1068, 2019.

[7] A. Nguyen, P. Pasquier, et D. Marcotte, « Thermal resistance and capacity model for standing column wells operating under a bleed control », Renewable Energy, vol. 76, p. 743-756, 2015.

[8] A. Nguyen, L. Jacques, and P. Pasquier, « An easy-to-use analytical model for standing column wells operating with bleed », *Applied Thermal Engineering*, vol. 258, 124543, 2025.

[9] L. Jacques, P. Pasquier, A. Nguyen, and G. Beaudry, « Improvement and experimental validation of an analytical model for standing column wells operated with bleed », *Applied Thermal Engineering*, vol. 279, 127620, 2025.

[10] L. Lamarche, *Fundamentals of Geothermal Heat Pump Systems: Design and Application*. Springer Nature Switzerland, 2023.

[11] G. Hellström, « Ground heat storage: thermal analyses of duct storage systems », Doctoral thesis, University of Lund, Sweden, 1991.

[12] S. Javed and J. D. Spitler, « Calculation of borehole thermal resistance », in *Advances in Ground-Source Heat Pump Systems*, Elsevier, 2016, p. 63-95.

[13] H. Zeng, N. Diao, and Z. Fang, « Heat transfer analysis of boreholes in vertical ground heat exchangers », *International Journal of Heat and Mass Transfer*, vol. 46, nº 23, p. 4467-4481, 2003.

[14] J. D. Spitler and S. E. A. Gehlin, « Thermal response testing for ground source heat pump systems—An historical review », *Renewable and Sustainable Energy Reviews*, vol. 50, p. 1125-1137, 2015.

[15] L. Lamarche, « Analytic models and effective resistances for coaxial ground heat exchangers », *Geothermics*, vol. 97, 102224, 2021.

[16] A.-M. Gustafsson and L. Westerlund, « Heat extraction thermal response test in groundwater-filled borehole heat exchanger – Investigation of the borehole thermal resistance », *Renewable Energy*, vol. 36, nº 9, p. 2388-2394, 2011.

[17] O. Todorov, K. Alanne, M. Virtanen, and R. Kosonen, « Different approaches for evaluation and modeling of the effective thermal resistance of groundwater-filled boreholes », *Energies*, vol. 14, nº 21, 6908, 2021.

[18] Z. Deng, « Modeling of standing column wells in ground source heat pump systems », Doctoral thesis, Oklahoma State University, USA, 2004.

[19] K. S. Chang, M. J. Kim, and Y. J. Kim, « An experimental study on the thermal performance evaluation of SCW ground heat exchanger », *International Journal of Air-Conditioning and Refrigeration*, vol. 25, nº 1, 1750006, 2017.

[20] K. S. Chang, Y. J. Kim, and M. J. Kim, « An investigation of hydrological effects on the thermal

performance of standing column well using the in-situ thermal response test », *International Journal of Air-Conditioning and Refrigeration*, 1950015, 2019.

[21] J. You and C. Lee, « Comparative analysis of geothermal energy in Korea based on closed borehole and single- and two-well standing column well geothermal heat exchange systems », *Applied Sciences*, vol. 10, nº 7, 2467, 2020.

[22] H. S. Carslaw and J. C. Jaeger, *Conduction of heat in solids*, 2th ed. Oxford: Clarendon Press, 1959.

[23] P. Mogensen, « Fluid to duct wall heat transfer in duct system heat storages », *Document-Swedish Council for Building Research*, nº 16, p. 652-657, 1983.

[24] F. P. Incropera, D. P. DeWitt, T. L. Bergman, and A. S. Lavine, *Fundamentals of heat and mass transfer*, 6th ed. Hoboken, NJ: Wiley, 2007.

[25] F. White, *Fluid Mechanics*, 7th ed. 2011.

[26] P. Pasquier and D. Marcotte, « Robust identification of volumetric heat capacity and analysis of thermal response tests by Bayesian inference with correlated residuals », *Applied Energy*, vol. 261, 114394, 2020.

[27] L. Jacques and P. Pasquier, « Obtaining the hydraulic and thermal properties of the main hydrostratigraphic units surrounding a standing column well using a thermal response test », *Journal of Hydrology*, vol. 623, 129823, 2023.

[28] M. Karamanis and F. Beutler, « Ensemble slice sampling: Parallel, black-box and gradient-free inference for correlated & multimodal distributions », *Statistics and Computing*, vol. 31, nº 5, p. 31-61, 2021.

[29] R. J. Moffat, « Describing the uncertainties in experimental results », Experimental thermal and fluid science, vol. 1, nº 1, p. 3-17, 1988.

[30] S. Robert, P. Pasquier, and A. Nguyen, « Impact of layered heterogeneity on thermal response test interpretation performed on a standing column well operated without bleed », *Geothermics*, vol. 101, 102353, 2022.